Optik 124 (2013) 4827–4831

Contents lists available at ScienceDirect

Optik

journal homepage: www.elsevier.de/ijleo

W doped SnO_2 growth via sol–gel routes and characterization: Nanocubes

Eyüp Fahri Keskenler[a,*], Güven Turgut[b], Serdar Aydın[b], Seydi Doğan[c]

[a] Recep Tayyip Erdoğan University, Faculty of Engineering, Department of Nanotechnology, 53100 Rize, Turkey
[b] Atatürk University, Kazım Karabekir Education Faculty, Department of Physics, 25240 Erzurum, Turkey
[c] Department of Electrical and Electronics Engineering, Faculty of Engineering and Architecture, Balikesir University, Balikesir 10145, Turkey

ARTICLE INFO

Article history:
Received 18 September 2012
Accepted 15 February 2013

Keywords:
SnO_2
W-doping
Nanocube
Sol–gel
Cubic phase

ABSTRACT

The effects of W doping on the characteristical properties of SnO_2 thin films prepared by sol–gel spin coating method were investigated. The SnO_2 thin films were deposited at various W doping ratios and characterized by various measurements. XRD studies indicated that the undoped and W doped SnO_2 films had cubic and tetragonal phases. The SEM images of WTO thin films showed cubic shaped nanocubes corresponding to cubic phase and the smaller particles corresponding to tetragonal phase were formed on the film surfaces, and their distributions and sizes were dependent on the W doping ratio. EDX spectroscopy analyses showed that the calculated and participated atomic ratios of W/(W + Sn) (at.%) in the starting solution and in the WTO thin films were almost close. It was found that the sheet resistance depended on W doping ratio and 2.0 at.% W doped SnO_2 (WTO) exhibited lowest value of sheet resistance ($7.11 \times 10^3\ \Omega/cm^2$).

1. Introduction

Tin oxide (SnO_2) has various application areas [1] due to its unique properties such as low electrical resistivity, high optical transmittance in the visible region, high infrared reflectivity, chemically inert and mechanically hard [2–5]. Some properties of SnO_2 thin films can be improved by suitable dopant elements such as antimony (Sb), fluorine (F), vanadium (V), and tungsten (W). Among these dopants, tungsten has oxidation states apt to W^{6+} ion state, and the radius of W^{6+} is close to that of Sn^{4+} (W^{6+}: 67 pm, Sn^{4+}: 71 pm), which make it easy to replace the Sn^{4+} ions. Therefore, tungsten-doped tin oxide may be expected to have a potential prospect [6].

Undoped and doped SnO_2 thin films have been prepared by various experimental techniques such as electrochemical deposition [7], hydrothermal method [8], polymerizing-complexing and sol–gel [9] techniques. However, to the best of our knowledge, the fabrication of W doped SnO_2 thin films have not been reported up to now by sol–gel spin coating method. Therefore, in this study, we aimed to investigate the effect of W doping on structural, morphological, optical and electrical properties of SnO_2 thin films prepared by sol–gel spin coating method.

2. Experimental

In the present study, W-doped tin oxide (WTO) thin films were prepared by sol–gel spin coating method on glass substrate using a sol prepared with stannous chloride dihydrate ($SnCl_2{\cdot}2H_2O$), tungsten hexachloride (WCl_6), monoethanolamine (C_2H_7NO, MEA) and 2-methoxyethanol ($C_3H_8O_2$, 2-MTE), as starting material, dopant source, stabilizer, and solvent, respectively. The molar ratio of MEA to metal salts was maintained at 1:1 in all solutions. Various amounts of the stannous chloride dihydrate and tugsten hexachloride were combined to achieve different W/W + Sn atomic ratios changing from 1.0 at.% to 4.0 at.% with 1.0 at.% step. The precursor sol was stirred at 80 °C for 24 h in a tightly closed flask to obtain a clear and homogenous solution. The glass substrates firstly were kept in boiling chromic acid solution and then they were rinsed with deionized water. Finally, they were cleaned with acetone, methanol and deionized water by using an ultrasonic cleaner and dried with nitrogen. The resultant solution being dropped on glass substrate was rotated at a speed of 3000 rpm for 30 s by using a spin-coater. After the glass substrates were coated, they were sintered at 200 °C for 5 min to evaporate solvent and remove the organic sediments and then spontaneously cooled to room temperature. This procedure was repeated for 4 times and finally, the samples were annealed in air at 450 °C for 30 min.

The structural characterization of the WTO thin films was carried out by X-ray diffraction (XRD) measurements using a Rigaku Miniflex II diffractometer with Cu Kα radiation (λ = 1.5418 Å). The diffractometer reflections were taken at room temperature and the values of 2θ were altered between 15° and 80°. Morphological properties of the W-doped SnO_2 thin films were determined

* Corresponding author. Tel.: +90 0464 223 6126x1764; fax: +90 0537 610 4849.
E-mail address: keskenler@gmail.com (E.F. Keskenler).

0030-4026/$ – see front matter © 2013 Elsevier GmbH. All rights reserved.
http://dx.doi.org/10.1016/j.ijleo.2013.02.038

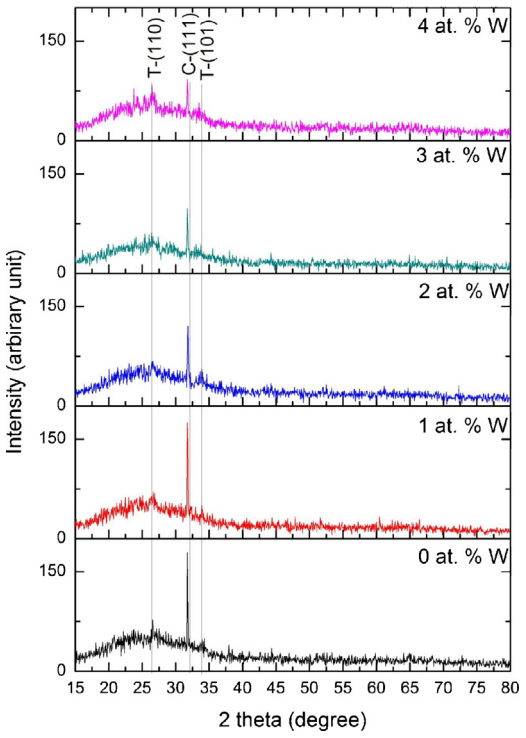

Fig. 1. XRD spectra for undoped and W doped SnO_2 thin films.

with Jeol Nano-SEM. The optical transmittance of the samples was recorded in spectral region of 300–1000 nm at 300 K using a UV-Vis spectrophotometer (Perkin-Elmer, Lambda 40) which works in the range of 200–1100 nm. The sheet resistance values of films were measured by means of four point probe technique.

3. Results and discussion

3.1. X-ray diffraction results

The crystal structure of WTO thin films was investigated by X-ray diffraction (XRD) patterns. Fig. 1 shows XRD spectra of WTO thin films. These spectra indicate that the samples have (1 1 1) plane corresponding to SnO_2 cubic phase (JPDS 50-1429) and (1 1 0), (1 0 1) planes corresponding to SnO_2 tetragonal rutile phase (JPDS 41-1445). No additional peak which implies oxides of tungsten were not observed. As seen in Fig. 1, the strongest orientation is (1 1 1) line of cubic structure and (1 1 1) peak intensity value of undoped sample has decreased continuously with increasing W dopant content. It can easily be concluded that the crystalline of WTO thin films are being deteriorated by increased W content.

Although SnO_2 crystallize in the tetragonal rutile crystal system, there are also orthorhombic and cubic phases of SnO_2. As a mineral, SnO_2 being formed at tetragonal rutile phase is also called Cassiterite [10]. Suito et al. [11] reported the phase transition from tetragonal to orthrombic structure. Shieh [12], Haines and Legér [13] observed SnO_2 cubic phase. Phase transformations of SnO_2 have usually been studied under high pressure. Jiang et al. [14] have found fluorite cubic phase with Fm3m space group above 18 GPa pressure, and Ono et al. [15] have observed peaks of (1 1 1), (2 0 0), (2 2 0), (2 2 2) belonging to the cubic structure under high pressure and temperature (about 23 GPa and 1000 K). In recent years, cubic and other phases have been reported from the experiments studies based on the solutions performed at atmospheric pressure [16–18]. Cubic phase for SnO_2 thin films prepared by reactive radio frequency magnetron sputtering with different sputtering power (about >100 W) have been reported by the Song et al. [19].

In this study, SnO_2 cubic structure has been obtained at atmospheric pressure, and to the best our knowledge, this is the first result obtained for SnO_2 films grown by the sol gel technique. In the literature, ethanole [20,21], 1-propyl alcohol [22], mixture of water and alcohol [23,24] are generally used as a solvent for preparation of SnO_2 films via sol–gel route. Huang et al. [25] have synthesized W doped SnO_2 thin film from sol–gel solution prepared by mixing a weighed quantity of $SnCl_2{\cdot}2H_2O$ with an ethanol/water, WCl_6 soluted in mixture. The reason for obtaining the cubic structure in this study may, at first, be the usage of a sol prepared with stannous chloride dihydrate ($SnCl_2{\cdot}2H_2O$), tungsten hexachloride (WCl_6), monoethanolamine (C_2H_7NO, MEA) and 2-methoxyethanol ($C_3H_8O_2$), as starting material, dopant source, stabilizer and solvent, respectively.

For the samples, the observed '*d*' values which are the interplaner distances are presented in Table 1 and these values are compared with the standard ones from the JPDS 50-1429 data files. The lattice constant '*a*' for cubic structure is determined by relation [26].

$$\frac{1}{d^2} = \left(\frac{h^2 + k^2 + l^2}{a^2}\right) \quad (1)$$

where ($h\,k\,l$) is miller indices. The calculated and standard lattice constants are also given in Table 1. The calculated '*a*' values agree with JPCDS card no: 50-1429 (a = 4.87 Å). As can be seen in Table 1, the lattice constant value for undoped sample is 4.8745 Å. This value decreases with W doping up to 2.0 at.%, and then it increases continuously with the W doping concentration in the films. This can be explained if it is considered that: W has many oxidation states such as +6, +5, +4, +3, +2 [27,28] and with decreasing the oxidation number of W, its ionic radii increases [28,29]. At the low doping levels, W^{6+} presumably substitutes with the Sn^{4+} and causes lattice constant decrease. With the increasing of W doping level in SnO_2 lattice, $W^{5,4,3,2+}$ oxidation states also substitute to Sn^{4+} and having increase in lattice constant. Similarly, in earlier studies, it was found that some of the Sn^{4+} ions in the lattice were replaced by Sb^{5+} at low doping level, however Sb^{3+} substituted to Sn^{4+} at high doping level [20].

3.2. SEM and EDX results

The composition of WTO thin films was determined by energy dispersive X-ray spectroscopy (EDX). EDX spectra of WTO thin films and the composition of elements in SnO_2 structure are together given in Fig. 2. These spectra clearly confirm the existence of Sn and W elements in the WTO thin films. The Si, Na, Mg and Ca ele-

Table 1
The structural, electrical and optical values of undoped and WTO thin films.

Sample	Cubic ($h\,k\,l$)	Cubic-d st. (Å)	Cubic-d obs. (Å)	Cubic-a (Å)	R_s ($\times 10^3$ Ω/cm^2)	E_g (eV)
Undoped SnO_2	(1 1 1)	2.8120	2.8143	4.8745	48.22	4.105
1.0 at.% W doped SnO_2	(1 1 1)	2.8120	2.8140	4.8739	12.96	4.112
2.0 at.% W doped SnO_2	(1 1 1)	2.8120	2.8236	4. 8626	7.11	4.115
3.0 at.% W doped SnO_2	(1 1 1)	2.8120	2.8146	4.8750	8.24	4.099
4.0 at.% W doped SnO_2	(1 1 1)	2.8120	2.8222	4.8852	9.60	4.097

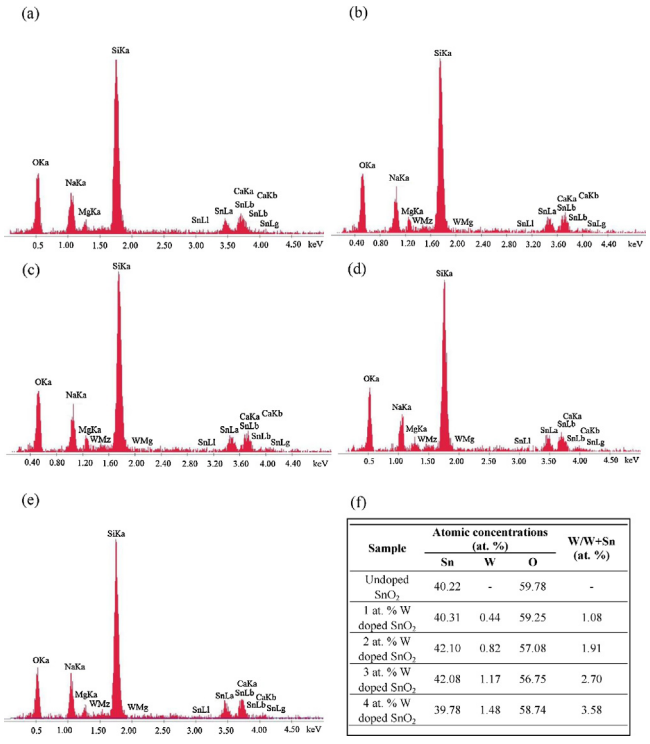

Sample	Atomic concentrations (at. %)			W/W+Sn (at. %)
	Sn	W	O	
Undoped SnO_2	40.22	-	59.78	-
1 at. % W doped SnO_2	40.31	0.44	59.25	1.08
2 at. % W doped SnO_2	42.10	0.82	57.08	1.91
3 at. % W doped SnO_2	42.08	1.17	56.75	2.70
4 at. % W doped SnO_2	39.78	1.48	58.74	3.58

Fig. 2. Energy dispersive spectroscopy analysis of W doped SnO_2 thin films: (a) undoped, (b) 1.0 at.% W doped, (c) 2.0 at.% W doped, (d) 3.0 at.% W doped, (e) 4.0 at.% W doped, (f) elemental concentrations in the film with different W doping levels in SnO_2 lattice.

ments, in solid films, are resulted from the glass substrates. EDX analyses show that the calculated and participated atomic ratios of W/(W + Sn) (at.%) in the starting solution and in the WTO thin films are almost close. These results confirm the reliability of the sol–gel spin coating method used in experiments. The scanning electron microscopy (SEM) images of WTOs thin films given in Fig. 3. It can be seen that the cubic shaped nanocubes are formed on surfaces of the films, and their distributions and sizes of nanocubes depend on the W doping ratio. For the undoped sample (Fig. 3a), the sizes of cubic nanoshape vary between 300 and 400 nm. For the 1.0 at.% W doped SnO_2 (Fig. 3b), the sizes of nanocubes decrease to the value of about 250–350 nm. As can be seen from Fig. 3c, the sizes of nanocubes sharply decrease to about 70 nm for the 2.0 at.% W doped SnO_2 and distribution of nanocubes is more arranged compared to undoped and 1.0 at.% W doped SnO_2. Above 2.0 at.% W doping level (Fig. 3d and e), the sizes of nanocubes increase sharply to about 200–250 nm and the film surface consist of lot of non-uniformed distorted nanocube shapes. Also, for the all samples, it should be noted that these nanocubes can be formed by an aggregation of small particles observed on glass substrates. These results are in harmony with tendency of lattice constant '*a*' calculated from XRD results for the WTO thin films. The similar structures of SnO_2 cubic phase and cubic shape were obtained for the films grown by hydrothermal method [8].

3.3. Electrical and optical properties

Electrical properties of the films were investigated by four point probe method. As can be seen in Table 1, there is a decrease in the sheet resistance values up to 2.0 at.% W doping levels, then it increases with W-dopant concentration increase. The variation in the sheet resistance of SnO_2 with W doping can be explained on the basis of the presence of different valance state of W element. When it is doped with W, some of the Sn^{4+} ions in the lattice can

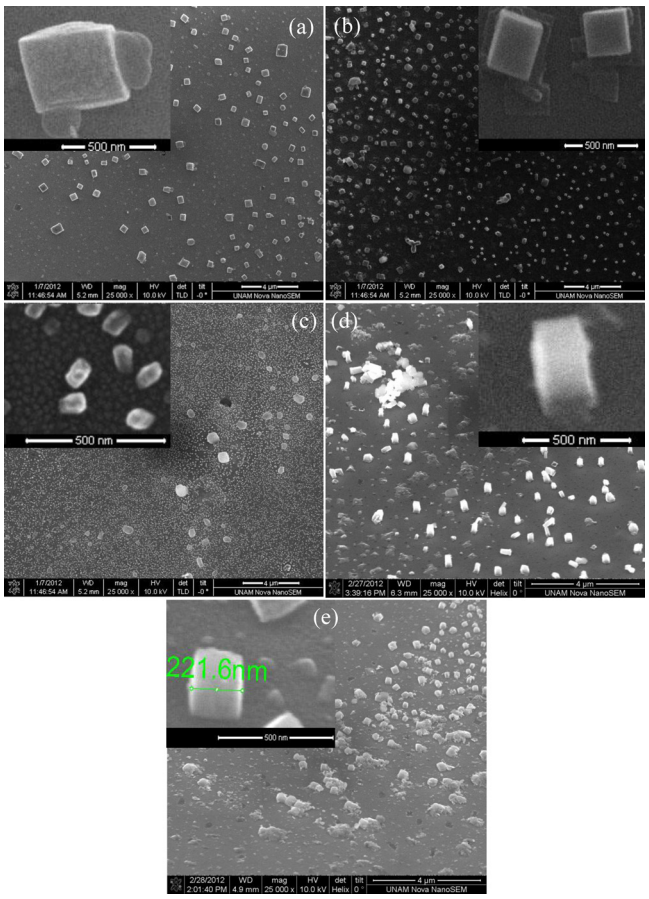

Fig. 3. SEM images undoped and W doped SnO_2 thin films: (a) undoped, (b) 1.0 at.% W doped, (c) 2.0 at.% W doped, (d) 3.0 at.% W doped, (e) 4.0 at.% W doped.

be replaced by W^{6+}, resulting the sheet resistance [6,25,30]. Hence, a reduction in the sheet resistance is observed until the W doping level reaches 2.0 at.%. Beyond 2.0 at.% of W doping, a part of the W^{6+} ions are reduced to the low valance states such as W^{4+}, W^{3+}, W^{2+}, resulting in the formation of acceptor states and a loss of carriers. Thus an increasing is observed at sheet resistance. In earlier studies, it was found that 3.0 at.% W doping reduced the sheet resistance of SnO_2 and W atoms were fully oxidized to the valence of 6+, and most of W^{6+} were incorporated inside the SnO_2 structure at low doping ratio from XPS study [6,25,30].

The optical properties of WTO thin films were investigated by using UV-Vis spectrophotometer. Transmittance spectra are given in Fig. 4. As can be seen, the transmittance values are varied

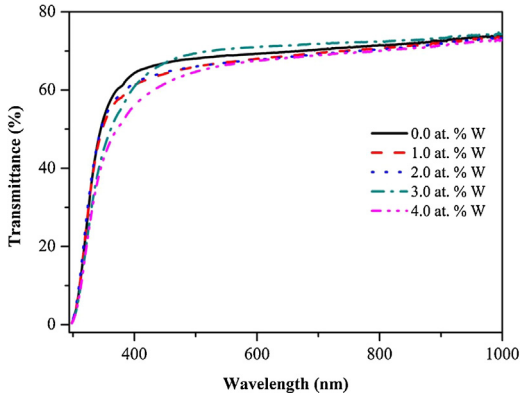

Fig. 4. Transmittance spectra for undoped and W doped SnO_2 thin films.

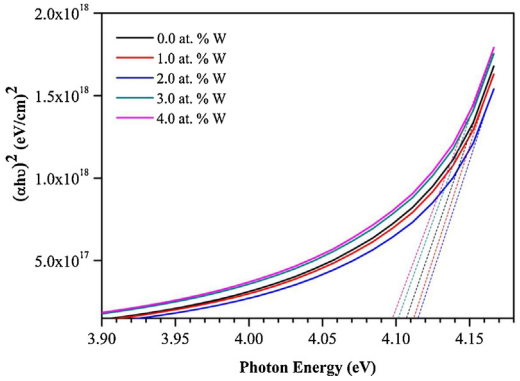

Fig. 5. The variation of $(\alpha h\nu)^2$ vs. $h\nu$ for undoped and W doped SnO_2 thin films.

between 60 and 75% in visible region. It is quite clear from the transmittance spectra that transparency has slightly changed with W doping. The analysis of the dependence of absorption coefficient versus photon energy in the high absorption regions is carried out to obtain more detailed information about the energy band gaps. The absorption coefficient (α) is determined by the equation [31];

$$\alpha = \frac{\ln(1/T)}{d} \quad (2)$$

where T is transmission and d is film thickness. The optical band gap of WTOs is obtained by following relation [32];

$$\alpha h\nu = A(h\nu - E_g)^{1/2} \quad (3)$$

where $h\nu$ and A are photon energy and the constant, respectively. E_g values were determined by plotting $(\alpha h\nu)^2$ vs. $h\nu$ and extrapolating of the linear region of the plot to zero absorption ($(\alpha h\nu)^2 = 0$). The band gap values of undoped, 1.0, 2.0, 3.0 and 4.0 at.% W doped SnO_2 thin films were found as 4.105, 4.112, 4.115, 4.099, 4.097 eV, respectively. It is clearly seen in Fig. 5 that the increasing W content in the SnO_2 structures up to 2.0 at.%, the band gap values increase and then continuously decrease with further increasing W doping level. The reason for increasing band gap with W content may probably be explained as follows; SnO_2 is one of degenerate semiconductors [10], which the Fermi level lies within the conduction band [27]. Thus, the optical band gaps are related to the excitation of the electrons from the valance band to Fermi levels [33,34]. This means that Fermi level is lifted some more into the conduction band of the degenerate semiconductor due to the increase in the carrier density. This leads to the energy band broadening (shifting) and some of the Sn^{4+} ions in the lattice are replaced by W^{6+} (or W^{5+}), and this is called Moss–Burstein effect [35]. A decrease in the energy band gaps beyond 2.0 at.% W doping can be caused that a part of the W^{6+} ions is reduced to lower valance states of W like W^{4+}, W^{3+}, W^{2+}, which can result in the formation of defects, impurities or completely not substitution of dopant with host atoms or interstitial and lattice strain [36–39]. The calculated lattice constant values support that W^{6+} are being replaced with Sn^{4+} at low doping contents (for 1.0 and 2.0 at.%).

4. Conclusions

This study presents cubic phase being obtained for the first time for W doped SnO_2 thin films grown by sol–gel spin coating, using methanolamine, 2-methoxyethanol, stannous chloride dihydrate, and tungsten hexachloride based on precursor solution. XRD studies indicate that the undoped and W doped SnO_2 have grown at cubic and tetragonal phases. EDX analyses show that the calculated and participated atomic ratios of W/(W + Sn) (at.%) in the starting solution and in the WTO thin films are almost close. The SEM images of WTOs thin films showed that the various distributed and sized cubic shaped nanocubes were formed on the surfaces of the films, depending on W doping ratio. All results had showed that 2.0 at.% W doped SnO_2 film had the best optoelectronic property. Thus, the results of this study indicate that the structural, morphological, electrical, and optical properties of the SnO_2 thin films prepared by sol–gel method can be strongly affected by the incorporation of W elements in SnO_2 thin films and WTO thin films can be useful for micro and nano-sized optoelectronic device applications.

References

[1] D. Jadsadapattarakul, C. Euvananont, C. Thanachayanont, J. Nukeaw, T. Sooknoi, Tin oxide thin films deposited by ultrasonic spray pyrolysis, Ceram. Int. 34 (2008) 1051–1054.
[2] E. Elangovan, S.A. Shivashankar, K. Ramamurthi, Studies on structural and electrical properties of sprayed SnO_2:Sb films, J. Cryst. Growth 276 (2005) 215–221.
[3] K.S. Kim, S.Y. Yoon, W.J. Lee, K.H. Kim, Surface morphologies and electrical properties of antimony-doped tin oxide films deposited by plasma-enhanced chemical vapor deposition, Surf. Coat. Technol. 138 (2001) 229–236.
[4] S. Chacko, N.S. Philip, K.G. Gopchandran, P. Koshy, V.K. Vaidyan, Nanostructural and surface morphological evolution of chemically sprayed SnO_2 thin films, Appl. Surf. Chem. 254 (2008) 2179–2186.
[5] E. Elangovan, M.P. Singh, K. Ramamurthi, Studies on structural and electrical properties of spray deposited SnO_2:F thin films as a function of film thickness, Mater. Sci. Eng. B 113 (2004) 143–148.
[6] Y. Huang, Q. Zhan, G. Li, Transparent conductive tungsten-doped tin oxide polycrystalline films prepared on quartz substrates, Semicond. Sci. Technol. 24 (2009), 015003-5.
[7] M. Lai, J.H. Lim, S. Mubeen, Y. Rheem, A. Mulchandani, M.A. Deshusses, N.V. Myung, Size-controlled electrochemical synthesis and properties of SnO_2 nanotubes, Nanotechnology 20 (2009), 185602-6.
[8] L. Shi, K. Bao, J. Cao, Y. Qian, Controlled fabrication of SnO_2 solid and hollow nanocubes with a simple hydrothermal route, Appl. Phys. Lett. 93 (2008) 152511.
[9] M. Bagheri-Mohagheghi, N. Shahtahmasebi, M.R. Alinejad, A. Youssefi, M. Shokooh-Sarem, The effect of the post-annealing temperature on the nanostructure and energy band gap of Sno_2 semiconducting oxide nano-particles synthesized by polymerizing-complexing sol–gel method, Physica B 403 (2008) 2431–2437.
[10] M. Batzill, U. Diebold, The surface and materials science of tin oxide, Prog. Surf. Sci. 79 (2005) 47–154.
[11] K. Suito, N. Kawai, Y. Masuda, High pressure synthesis of orthorhombic SnO_2, Mater. Res. Bull. 10 (1975) 677–680.
[12] A.R. Shien, High-pressure phases in SnO_2 to 117 GPa, Phys. Rev. B 73 (2006), 014105-7.
[13] J. Haines, J.M. Legér, X-ray diffraction study of the phase transitions and structural evolution of tin dioxide at high pressure: relationships between structure types and implications for other rutile-type dioxides, Phys. Rev. B 55 (1997) 1144–1154.
[14] J.Z. Jiang, L. Gerward, J.S. Olsen, Pressure induced phase transformation in nanocrystal SnO_2, Scr. Mater. 44 (2001) 1983–1986.
[15] S. Ono, E. Ito, T. Katsura, A. Yoneda, M.J. Walter, S. Urakawa, W. Utsumi, K. Funakoshi, Thermoelastic properties of high-pressure phase of SnO_2 determined by in situ X-ray observations up to 30 GPa and 1400 K, Phys. Chem. Miner. 27 (2000) 618–622.
[16] P.S. Patil, R.K. Kawar, S.B. Sadale, P.S. Chigare, Properties of spray deposited tin oxide thin films derived from tri-n-butyltin acetate, Thin Solid Films 437 (2003) 34–44.
[17] C. Agashe, R.C. Aiyer, High-yield synthesis of nanocrystalline tin dioxide by thermal decomposition for use in gas sensors, Int. J. Appl. Ceram. Technol. 5 (2008) 181–187.
[18] B. Hariprakash, A.U. Mane, S.K. Martha, S.A. Gaffoor, S.A. Shivashankar, A.K. Shukla, A low-cost, high energy-density lead-acid battery, Electrochem. Solid State Lett. 7 (2004) A66–A69.
[19] J. Song, M.Z. Cai, Q.F. Dong, M.S. Zhen, Q.H. Wu, S.T. Wu, Structural and electrochemical characterization of SnO_x thin films for Li-ion microbattery, Electrochim. Acta 54 (2009) 2748–2753.
[20] C. Terrier, J.P. Chatelon, J.A. Roger, R. Berjoan, C. Dubois, Analysis of antimony doping in tin oxide thin films obtained by the sol–gel method, J. Sol–Gel Sci. Technol. 10 (1997) 75–81.
[21] Y.J. Lin, C.J. Wu, The properties of antimony-doped tin oxide thin films from the sol–gel process, Surf. Coat. Technol. 88 (1997) 239–247.
[22] M. Izerrouken, S. Kermadi, N. Souami, A. Sari, M. Boumaour, Influence of reactor neutrons irradiation on electrical, optical and structural properties of SnO_2 film prepared by sol–gel method, Nucl. Instrum. Methods A 611 (2009) 14–17.
[23] Y. Xiao, S. Ge, L. Xi, Y. Zuo, X. Zhou, B. Zhang, L. Zhang, C. Li, X. Han, Z. Wen, Room temperature ferromagnetism of Mn-doped SnO_2 thin films fabricated by sol–gel method, Appl. Surf. Sci. 254 (2008) 7459–7463.
[24] L.K. Dua, A. De, S. Chakraborty, P.K. Biswas, Study of spin coated high antimony content Sn–Sb oxide films on silica glass, Mater. Charact. 59 (2008) 578–586.

[25] Y. Huang, D. Li, J. Feng, G. Li, Q. Zhang, Transparent conductive tungsten-doped tin oxide thin films synthesized by sol–gel technique on quartz glass substrates, J. Sol–Gel Sci. Technol. 54 (2010) 276–281.
[26] R.J.D. Tilley, Crystal and Crystal Structures, Wiley, London, UK, 2006.
[27] J.J. Lingane, L.A. Small, Polarography of the various oxidation states of tungsten, J. Am. Chem. Soc. 71 (1949) 973–978.
[28] E. Lassner, W.-D. Schubert, Tungsten, Kluwer Academic, New York, 1999.
[29] N.N. Greenwood, A. Earnsha, Chemistry of the Elements, second ed., Elseiver, Oxford, UK, 1997.
[30] Y. Huang, G. Li, J. Feng, Q. Zhang, Investigation on structural, electrical and optical properties of tungsten-doped tin oxide thin films, Thin Solid Films 518 (2010) 1892–1896.
[31] T. Serin, N. Serin, S. Karadeniz, H. Sarı, N. Tuğluoğlu, O. Pakma, Electrical, structural and optical properties of SnO_2 thin films prepared by spray pyrolysis, J. Non-Cryst. Solids 352 (2006) 209–215.
[32] J. Tauc, R. Grigorovici, A. Vancu, Optical properties and electronic structure of amorphous germanium, Phys. Status Solidi (b) 15 (1966) 627–637.
[33] A.R. Babar, S.S. Shinde, A.V. Moholkar, C.H. Bhosale, J.H. Kim, K.Y. Rajpure, Structural and optoelectronic properties of antimony incorporated tin oxide thin films, J. Alloys Compd. 505 (2010) 416–422.
[34] A.R. Babar, S.S. Shinde, A.V. Moholkar, C.H. Bhosale, J.H. Kim, K.Y. Rajpure, Sensing properties of sprayed antimony doped tin oxide thin films: solution molarity, J. Alloys Compd. 509 (2011) 3108–3115.
[35] E. Burstein, Anomalous optical absorption limit in InSb, Phys. Rev. 93 (1954) 632–633.
[36] F. Yakuphanoglu, Y. Caglar, S. Ilican, M. Caglar, The effects of fluorine on the structural, surface morphology and optical properties of ZnO thin films, Physica B 394 (2007) 86–92.
[37] M. Tomakin, M. Altunbas, E. Bacaksız, I. Polat, Preparation and characterization of new window material CdS thin films at low substrate temperature (<300 K) with vacuum deposition, Mater. Sci. Semicond. Process. 14 (2011) 120–127.
[38] L.B. Freund, S. Suresh, Thin Film Materials: Stress, Defect Formation and Surface Evolution, Cambridge University Press, Cambridge, 2003, pp. 192.
[39] Y.H. Lee, W.J. Lee, Y.S. Kwon, G.Y. Yeom, J.K. Yoon, Effects of CdS substrates on the physical properties of polycrystalline CdTe films, Thin Solid Films 341 (1999) 172–175.